

# Drop Impact on a Vibrated, Heated Surface: Towards a Potential New Way of Elaborating Nuclear Fuel from Gel Microspheres

Méryl Brothier, Dominique Moulinier and Christophe Bertaux

**Abstract**—The gel-supported precipitation (GSP) process can be used to make spherical particles (spherules) of nuclear fuel, particularly for very high temperature reactors (VHTR) and even for implementing the process called SPHEREPAC. In these different cases, the main characteristics are the sphericity of the particles to be manufactured and the control over their grain size. Nonetheless, depending on the specifications defined for these spherical particles, the GSP process has intrinsic limits, particularly when fabricating very small particles. This paper describes the use of secondary fragmentation (water, water/PVA and uranyl nitrate) on solid surfaces under varying temperature and vibration conditions to assess the relevance of using this new technique to manufacture very small spherical particles by means of a modified GSP process. The fragmentation mechanisms are monitored and analysed, before the trends for its subsequent optimised application are described.

**Keywords**—Microsphere elaboration, nuclear fuel, droplet impact, gel-supported precipitation process.

## I. INTRODUCTION

SEVERAL types of nuclear applications require using actinide oxide spherules, i.e. for manufacturing VHTR-type fuels or for implementing processes such as the Spherical [1] or Sphere-pac process [2]. A standard method for elaborating spherules is based on the GSP process (see Fig. 1). However, it is proving problematic to obtain relatively small particle sizes (diameters typically under 100  $\mu\text{m}$ ) with the latest standard version of this process. One of the disadvantages of this process is the method used to generate droplets prior to precipitation. The fact that very small injector diameters are used tends to result in spurious blockage. Certain changes have been recommended by various authors to avoid this problem, such as using a rotating disc to fractionate the liquid by centrifugation. Nonetheless, these devices are poorly adapted to viscous liquids and produce relatively high droplet velocities, which have a negative impact on controlling the sphericity of the droplets typically

obtained by precipitation in an ammonia bath.

Furthermore, being able to reach a degree of freedom in the grain size ranges via the GSP process would offer a potential advantage compared with the current technology relying on vibrating nozzles or rotating discs, which fixes *de facto* the target grain sizes (virtually necessary to replace the injectors according to the target characteristics of the spherules).

This study assesses another strategy for producing droplets, which are the forerunners needed to make spherules. More specifically, this paper focuses on the possibility of obtaining secondary fragmentation from aqueous solutions with or without actinides by orthogonal impact on solid surfaces.

The first part of this paper describes a novel method which couples temperature and vibrations as the potential parameters for controlling fractionation. The second part discusses its application to water (with or without additives) and then to uranyl nitrate. The final part of the document discusses the results and compares the different cases, offering future prospects in terms of the relevant orientations for the possible implementation of a spherule production process by droplet impact via the application of GSP.

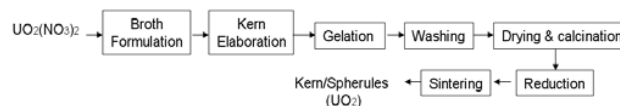


Fig. 1: Simplified diagram of the GSP process applied to  $\text{UO}_2$  spherule elaboration

## II. GSP PROCESS AND PRODUCING MICROSPHERES

Many process [1], [2] use gel-derived microspheres as feed material for nuclear fuel fabrication, particularly since they are free-flowing and dust-free, or simply because their shape is specified for particular applications. To produce these microspheres, several techniques are possible, in particular by internal or external gelation [3]-[4]. These processes have both advantages and drawbacks for which improvements have been proposed over the years. This includes studying the droplet properties before the precipitation stage since they impact the sphericity and the size of the particles obtained. Various ways of generating of these droplets can be noted and patents have been registered on topics focusing on controlling the droplet size and sphericity [5]-[6]. However these solutions are not fully satisfactory in the case of external gelation because they do not offer a simple, flexible way to change the size of the particles while controlling their

Méryl Brothier is with the Commissariat à l'Energie Atomique et aux Energies Alternatives, in the Fuel Research Department: CEA, DEN, DEC/SPUA/LCU, 13108 Saint Paul les Durance, France. (E-mail: meryl.brothier@cea.fr).

D. Moulinier is with the Commissariat à l'Energie Atomique et aux Energies Alternatives, in the Fuel Research Department: CEA, DEN, DEC/SPUA/LCU, 13108 Saint Paul les Durance, France. (E-mail: dominique.moulinier@cea.fr).

Ch. Bertaux is the Commissariat à l'Energie Atomique et aux Energies Alternatives, in the Fuel Research Department: CEA, DEN, DEC/SPUA/LCU, 13108 Saint Paul les Durance, France. (E-mail: christophe.bertaux@cea.fr).

sphericity and preventing the risk of nozzle blockage.

The difficulties associated with blocking are quite considerable in a nuclear process since they often involve penalising maintenance operations. Knowing that the diameter of droplets obtained by destabilising a jet through a vibrating nozzle strongly depends on the nozzle diameter (see Fig. 2), and in light of equation (1) (where  $d_0$  is mean diameter of the drop,  $Q$  the volume flow through the vibrating injector (depending on the injector diameter) and  $f$  the frequency of the vibrations), it is understandable that this way of generating droplets offers restricted possibilities due to blockage risks.

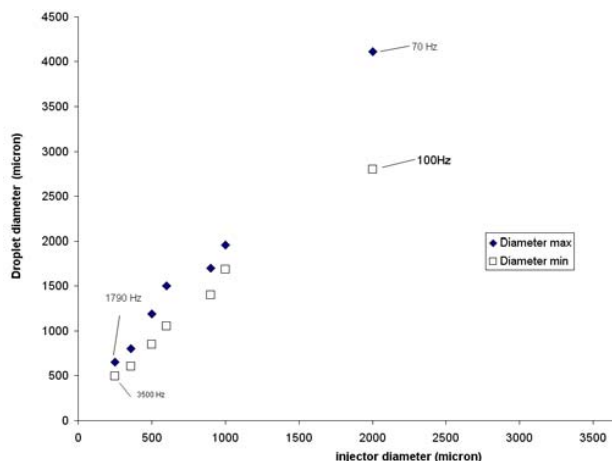


Fig. 2: Variation in the diameter of droplets obtained by passing through an aqueous PVA solution with a viscosity of 65 cP (18°C) via a vibrating injector with a variable-opening diameter. The diamonds show the maximum values obtained while the squares show the minimum values within a frequency range of 70 to 3.5 kHz.

This is why using centrifugation devices have been developed. Nevertheless, these devices generate droplets at relatively fast ejection velocities, which is penalising for their sphericity. The impact of droplets in the precipitation solution results in deformations that are sometimes unacceptable for the sphericity of the particles obtained after gelation.

$$d_0 = \sqrt[3]{\frac{6Q}{\pi \cdot f}} \quad (1)$$

This study assesses the possibility of using an innovative alternative to produce uranium oxide spherules (see Fig. 3) which is free of blockage risks and which controls the sphericity criterion, i.e. generating droplets before precipitation at low velocities to limit their flattening upon impact with the precipitation bath surfaces. This paper describes this strategy which is based on the fractionation of liquid droplets by their impact on a solid surface that is both heated and vibrating.

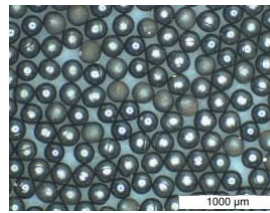


Fig. 3 : UO<sub>2</sub> spherule with a mean diameter close to 220  $\mu$ m elaborated by the GSP process

### III. DROPLET IMPACT ON A SOLID TARGET

Droplet impact on a solid target is a technique used in numerous applications, from fuel dispersion in engines to material coatings on parts and surfaces. There are a number of basic studies describing the phenomena involved and providing temporal representations of the spreading kinematics and sometimes even the splashing kinematics as a function of the impact conditions. Most of the models, however, are deficient in some way since they fail to take into account all of the influential parameters. In particular, the surface temperature and the surface condition are often neglected, while the splashing regime is often covered rather concisely, which makes it impossible to obtain sufficiently precise predictive models for any given case.

In the case discussed in this paper, a novel parameter has been taken into account to achieve an additional degree of freedom to control fractionation, i.e. vibration of the impacted surface. This is generally not covered in the literature, except for the rare paper investigating the fractionation of liquid films produced by centrifugation [8] which is why this paper aims at providing preliminary information on this potential method for generating micro-spherules by droplet impact on vibrating, heated surfaces.

#### A. Basic Phenomena and Preponderant Parameters

The impact of a droplet of a solid vibrating surface – heated or not – results in the simultaneous occurrence of numerous phenomena some of which are relatively complex. Several reviews ([9], [10], [11] and [12]) provide good descriptions of the main phenomena involved and their determining parameters, though very little information precisely describing the vibration conditions coupled with temperature are given for this specific case. A number of parameters taken into account separately are recalled below and will be considered in a simplified manner for the experimental cases under investigation:

- (i) Incidental droplet velocities
- (ii) Droplet diameter
- (iii) Physico-chemical properties of the liquid
- (iv) Properties of the surface.

The first contact between the base of the droplet and the solid surface is temporary for an ideal case and for an unheated solid surface. The shock wave and its propagation in the droplet after impacting a solid surface is shown in Figure 4 [11]. The relation between the impact velocity ( $U_i$ ) of the

droplet (whose the radius is noted  $R$ ), the contact edge velocity ( $U_e$ ) and the contact angle  $\beta$  is:

$$U_e = U_i / \tan \beta \quad (2)$$

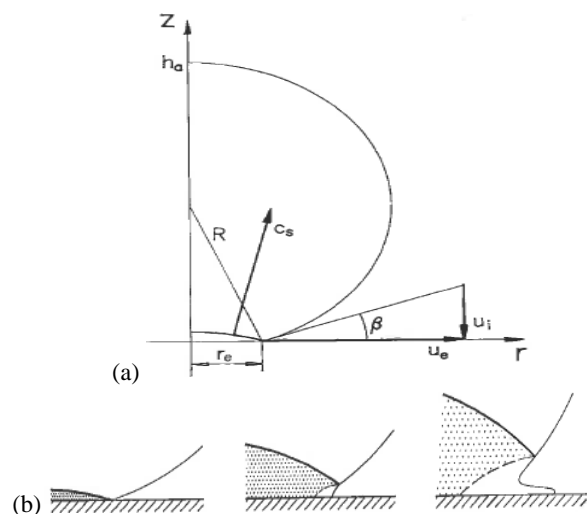


Fig. 4: Impact of a droplet on a solid surface: (a) initial stage, (b) propagation of a shock wave in the droplet after the initial step and its expansion until the onset of sideways jetting [11]

During the spreading of the droplet, a contact zone of radius  $r_e$  develops. The shock propagates inside the droplet with a velocity  $c_s$  whose the magnitude is of the same order as the sound speed in the liquid. The shock wave remains attached to the contact edge as long as the impact velocity is greater than the value of  $c_s \cdot \sin \beta$  and the liquid ahead of the shock is not yet disturbed by the impact. When the contact angle becomes higher than a critical angle called  $\beta_c$  (see equation 4) the shock wave separates from the contact edge and moves up the undisturbed surface. The compressed liquid zone (this enclosed by the shock wave and the solid surface) results in sideways jetting (Fig. 4 (b)).

$$\beta_c = \sin^{-1} (U_i / c_s) = \sin^{-1} Mi \quad (=4.38^\circ \text{ for water}) \quad (3)$$

where  $Mi$  is the impact Mach number ( $U_i/c$ ) and  $c$  the sound velocity in the liquid under investigation.

The time between impact and shock detachment ( $t_c$ ) can therefore be given by equation 5 where  $r$  represents the perfect gas constant [11]:

$$t_c \cdot c / R = \frac{1}{Mi} [1 - \cos(\sin^{-1} Mi)] \approx Mi / 2 \quad (4)$$

Spreading begins as soon as jetting starts. Spreading is greatly influenced by the kinetic energy of the droplet and by the impact velocity. The motion of the liquid leads to the formation of a thin liquid called lamella. If the impact velocity is sufficient, the jetting motion also leads to a disintegration of the liquid and splashing occurs (see section 2.3). During spreading, the kinetic and surface energy of the droplet are

dissipated by a viscous process in the thin sheet of liquid and are transformed into additional surface energy. Depending on the impact conditions, the film (called lamella) can fractionate into fingers and result in the formation of secondary droplets (the number of droplets is written  $N$ ) or in shrinkage to form smaller sizes.

The influence of the surface characteristics (temperature, roughness, etc.) is described in section 2.3. It is interesting to point out that the so-called Leidenfrost temperature can be a characteristic of the surface itself, the surface condition or the surface temperature. KJ. Baumeister [13] has studied this aspect and current research considers the impact surface by integrating data on the Leidenfrost temperature through the fact that the tested resistance level does not make it possible to reach this temperature (see Fig. 5). Tests to estimate the life span of droplets on silicone show that the Leidenfrost temperature is higher than the maximum acceptable temperature for the surface resistance. Figure 5 provides an estimate of the Leidenfrost temperature.

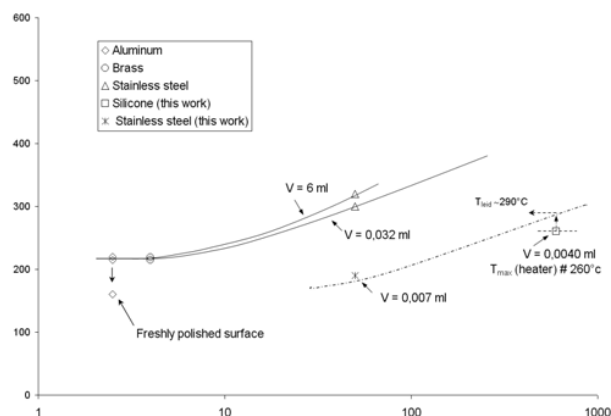


Fig. 5: Effect of the material nature and droplet volume on the Leidenfrost temperature: data extracted from [13] except data on the silicone case (square)  $\alpha$  and this with stainless steel using a small droplet diameter (0.007 ml)

### B. Representation of droplet spread factors upon impact

The radius of the liquid lamella scaled with the droplet radius is called the spread factor  $\zeta$  whose the maximal value ( $\zeta_m$ ) is reached at the end of the expansion phase. The authors provide different analytical representations of the variation in this spread factor as a function of time, as well as its maximum value.

This spread factor also depends on the viscosity of the liquid ( $\mu$ ), the liquid's density ( $\rho$ ), and the surface tension between both the liquid and the gas ( $\sigma_{lg}$ ) and the liquid and the surface ( $\sigma_{ls}$ ). In many representations, the effects due to gravity are negligible since the lamella is very thin. To take into account these parameters, dimensionless numbers are often used, such as the Weber number ( $We = \rho U_i^2 (Do) / \sigma_{lg}$ ) or the Reynolds number ( $Re = \rho Do U_i / \mu$ ). It should be pointed out that some results in the literature are discussed in terms of the Ohnesorge number ( $Oh$ ) and the splash number ( $K$ ), it being understood that  $Oh = We^{1/2} \cdot Re^{-1}$  and  $K = We^{1/2} \cdot Re^{1/4}$ .

TABLE I  
CORRELATIONS FOR SPREADING/SPLASHING CHARACTERISTICS OF IMPINGING DROPLETS ON A SOLID SURFACE

References:	Correlations	Notes
Bolle et al. [14]	$\zeta = 1,67 \cdot (3,1 \cdot \tau \cdot \tau^2)$	Theoretical model (valid for film boiling conditions and $0.2 \cdot Do / Ui \leq t \leq [1,2; 1,5] \cdot Do / Ui$ )
H.Y. Kim et al. [15] *	$\tau = t \cdot Ui / Do$ $\zeta = A \cdot t^{1/2}$	Analytical study A is dependent in particular on droplet impact conditions
Shi et al. [16]	$\zeta = 1,6Ui/Do \cdot \left[ t - (10^6 \nu)^{0,1} \cdot \frac{4\sigma Ui^{0,6} t^{2,95}}{\rho_l \cdot Do^3} \right]$ $\zeta = 1,6Ui^{1,1} \cdot \left[ t - \frac{6,8 \cdot \sigma Ui^{0,25} t^{2,95}}{\rho_l \cdot Do^3} \right] / Do$	Nucleate boiling conditions  Film boiling conditions
F. Akao et al. [17]	$\zeta_{\max} = 0,613 \cdot We^{0,39}$	Experimental correlation (copper surface) $2.1 \leq Do \leq 2.9 \text{ mm}$ $0.66 \leq Ui \leq 3.21 \text{ m.s}^{-1}$ $T_{\text{surface}} = 400^\circ\text{C}$
Kurokawa et al. [18]	$\zeta_{\max} = 0,96 \cdot Re^{0,095} \cdot We^{0,084}$	Experimental and numerical study Surface: glass $150 \leq We \leq 750$ $850 \leq Re \leq 50000$ $T_{\text{surface}} = 22^\circ\text{C}$
A.L. Biance et al. [19]	$\zeta_{\max} = We^{0,25}$	Experimental and analytical study $T = 280^\circ\text{C}$
R. Bhola et al. [20]	$N = \frac{K}{4 \cdot \sqrt{3}}$	Millimetric droplet Analytical study from consideration of an integral energy balance

With: Do :initial diameter of the droplet, Ui: velocity of the droplet just before impact, t the time after the impact,

Based on these different expressions, several representations of  $\zeta$ ,  $\zeta_m$  and N have been recommended by numerous authors. The correlations have been compared with the experimental results of this study and are shown in Table I.

### C. Splashing conditions and potential application to produce calibrated droplets for the fabrication of microspheres

Under specific conditions of impinging droplets, splashing can occur. According to reference [7], the splashing-deposition boundary takes place when the Ohnesorge number is higher than the value given by the following relation:

$$Oh_c = \sqrt{\frac{3(1 - \cos \beta) \xi_m^2 - 12}{Re^2 - 4,5 \xi_m^4 \cdot Re}} \quad (5)$$

Other authors have defined the boundaries between the different impact conditions (deposition, splashing, rebound). C. Mundo [7], for example, introduced the Sommerfeld parameter (K) which is used to define the boundaries between the different impact conditions for a cold, dry surface according to the expression  $Oh=f(Re)$  (see Fig. 6). The number  $K = 57.7$  has been identified as defining the boundary between splashing conditions and deposition conditions in the experiments conducted.

Some authors (see [21]) even include additional information to define these ranges, particularly taking into account the roughness of the impact surface (the average roughness of the solid surface to assess this parameter).

Nonetheless, the literature gives no general expression of K for all types of surfaces which are also heated and vibrating. This is why it is necessary to conduct specific experiments in our case, even if the above-mentioned studies may provide us with some information on the trends that can be expected.

The standard vibration approach used to fractionate a liquid pool is based on Faraday instability as illustrated in Figure 7. Rayleigh showed that the frequency of the wave formed on the surface of a liquid film deposited on a solid vibrating surface is sub-harmonic compared with the excitation frequency.

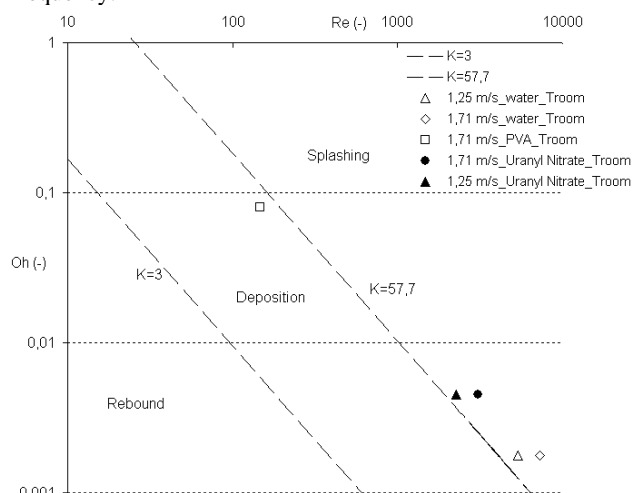


Fig. 6 : Empirical and theoretical correlations for incipient splashing

This study suggests combining vibrations and temperature

to estimate the effect on the control over the fractionating process. It should also be pointed out that the layer of liquid in this study is very thin and practically represents a limit case for taking into account the assumption of a free liquid surface. In the case of a droplet deposited on a surface at room temperature, the frequency of oscillation on the free surface under our experimental conditions is similar to the frequency imposed by the surface (see Fig. 8).

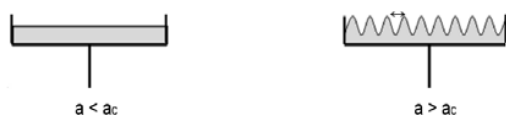


Fig. 7: Wave development under acceleration ( $a$ ) condition if  $a$  is higher than a critical value

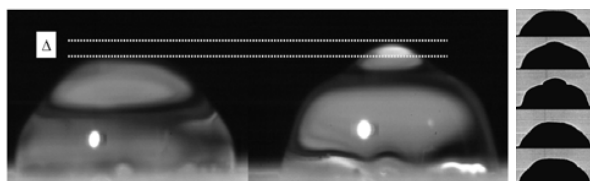


Fig. 8: Water droplet oscillation views on the studied vibrated surface (room temperature and frequency: 200 Hz; images on the right are taken every millisecond)

#### IV. MATERIALS AND METHODS

Figure 9 shows a schematic diagram of the experimental set-up used to record the deformation behavior of a single droplet impacting upon a heated vibrated solid surface. Syringes of different sizes produce droplets with diameters between 2 and 5 mm. The height measured from the impact liquid surface and the needle of the syringe ranges between 5 cm and 15 cm. This leads to a maximum terminal impact velocity of almost 1.7 m/s.

The droplet impact velocity was monitored prior to impact by a VM2-PHOTRON SA4 camera with a HMI light source. The impact and splashing were monitored by the same device. Perpendicular shots were taken at 45° or along the normal plane of the impact surface to track the spreading/ splashing phenomena and, where necessary, the number of fingers formed.

The droplet diameter was measured by scanning the picture just before impingement by comparison with an object of a known size. The accuracy of the speed and size was better than 5%.

The impact support comprised a stainless steel plate on which an 18 ohm silicone-cladded MINCO resistor was positioned. The average roughness of this surface was close to 0.1  $\mu\text{m}$  (Ra). This heater was feed by a current generator providing up to 20 Vcc. The maximum temperature imposed by the resistor was 260°C.

The impact support was vibrated by a shaker within a range between 0 and 1 kHz, with the amplitude capable of ranging between several micrometres and 0.5 cm.

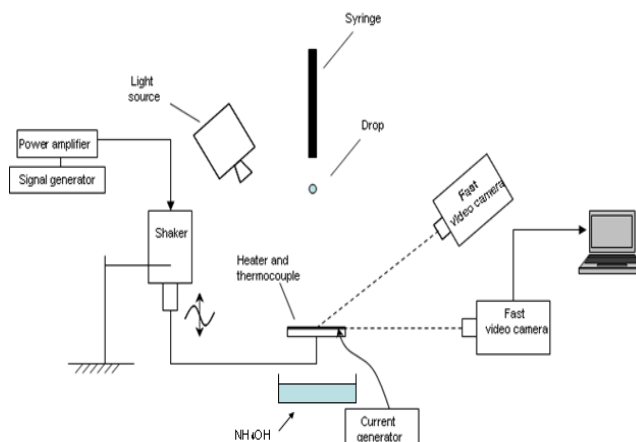


Fig. 9: Simplified diagram of the experimental set-up

The main uncertainties on the overall results of this study are given in Table II. Other than those already described, the calculation uncertainties are not shown in the graphic representations since the objective of this study is mainly to identify the conditions encouraging secondary fractionation and its control. Features of the liquid used for the impact study are given in Table III.

TABLE II  
MAIN UNCERTAINTIES

Parameter	Uncertainty
$U_i$	$\pm 0.1 \text{ m/s}$
$D_o$	$\pm 10\%$
$D$	$\pm 10\%$
$f$	$\pm 5\%$
$T$	$\pm 10^\circ\text{C}$
$N$	$\pm 2$

TABLE III  
CONSIDERED VALUES FOR LIQUIDS PROPERTIES AT 20°C

Liquid :	Masse volumique $\rho$ ( $\text{kg.m}^{-3}$ )	Viscosity $\mu$ (Pa.s)	Tension superficielle $\sigma$ ( $\text{N.m}^{-1}$ )
Water	1000	$1.10^{-3}$	$70.10^{-3}$
PVA/Water*	1020	$3.10^{-3}$	$70.10^{-3}$
Uranyl Nitrate	1150	$3.10^{-3}$	$80.10^{-3}$

\* PVA/water : Poly Vinylic Alcohol in aqueous solution.

#### V. RESULTS AND DISCUSSIONS

The first part of this section is dedicated to showing the characteristics (both qualitative and quantitative) of the deposition and the secondary atomization produced after the impact of a single liquid droplet onto a surface vibrated and heated. After this step, the main results are discussed by examining the expected phenomena and comparing with various types of liquid in order to change the properties which

greatly impact both deposition and atomization, knowing however that the device used for this study was not adapted to strongly vary the initial velocity of the droplet before its impact.

#### A. Droplet impact observations

As previously defined (see section 4), the typical time required for lamella detachment and formation is relatively short. It is about 0.5 ms for water. This study is not looking to precisely characterise detachment but to use it as a way of calibrating the number of images per second that may be defined for the high-speed camera described in section IV. Data was acquired at speeds of around 2,000 to 10,000 images per second. Two illustrations monitoring the impact and deposition phase of the liquids are given in Figure 10. Top and side views made it possible to observe spreading through the parameter  $\zeta$  and the number of fingers formed (N).

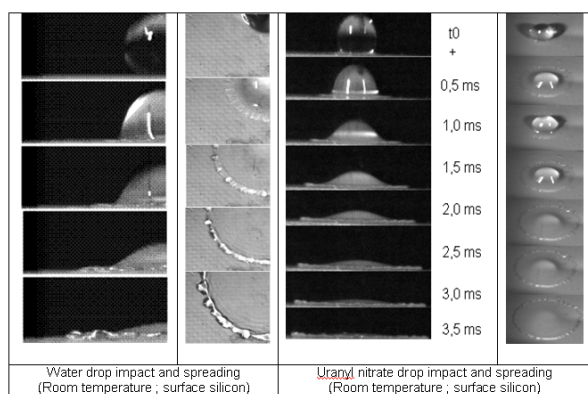


Fig. 10: Deposition of water and uranyl nitrate droplets with  $Re \sim 7300$  and  $Re \sim 3100$  on a silicone surface

These observations can be converted into curves that show spreading as a function of dimensionless time ( $\tau$ ) defined as described in Table I. The resulting figure (Fig. 11) thus provides information on the spreading kinetics for all three cases investigated (water, water/PVA and uranyl nitrate). It can be seen that the greatest spreading was obtained with uranyl nitrate at the maximum acceptable temperature for the silicone surface ( $260^\circ\text{C}$ ) and at a frequency of 80 Hz. The most relevant correlations for the conditions under investigation are provided by Kim and Boyle.

Vibration seems to have no significant effect on the spreading factor under the tested conditions. As mentioned in section C of this part, however, secondary atomization is more sensitive to this parameter.

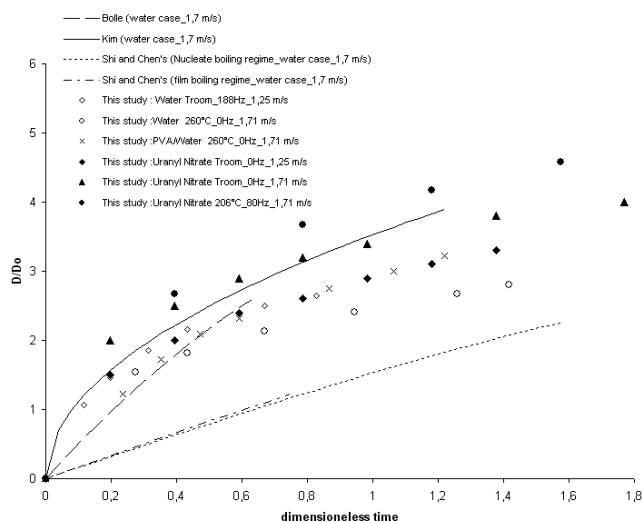


Fig. 11: Spreading for various studied cases as a function of the dimensionless time

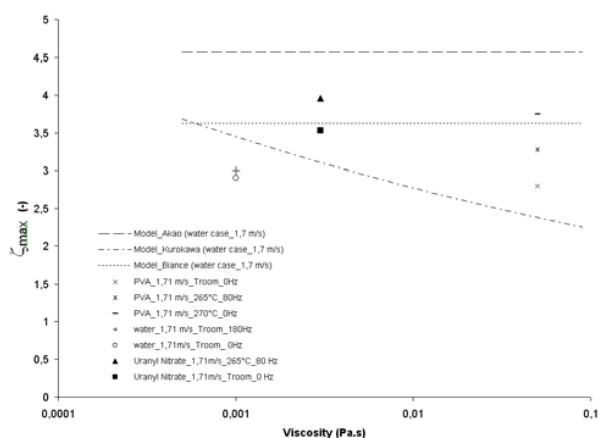


Fig. 12: Maximal values of  $\zeta_{\max}$  as a function of the viscosity

The viscosity is not a predominant parameter on the values of  $\zeta_{\max}$  in the range of tested conditions (Fig. 12). Nor does the number N seem to be strongly impacted by the temperature of the surface (see Fig. 13). The correlations used to predict the values of  $\zeta_{\max}$  and N for the conditions under investigation are relatively good, excepting that resulting from the Akao model which considerably overestimates  $\zeta_{\max}$ .

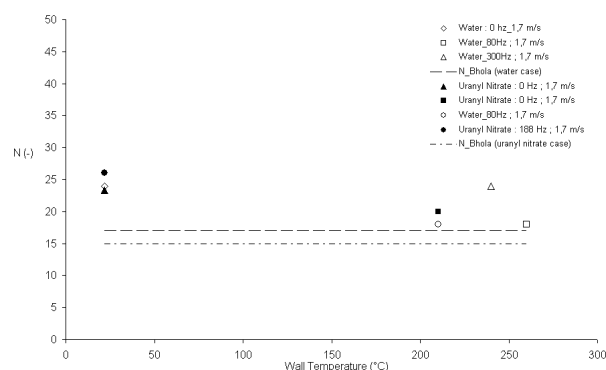


Fig. 13: Number of fingers formed during the spreading on a vibrated heated silicone surface

### B. Analysis impact conditions

The impact conditions of this study can be characterised by several types of analyses as mentioned in section III. Figure 6 shows the position of the impact conditions in a Re-Oh space. The number  $K$  is close to the critical value specified by C. Mundo [7] at ambient temperature. This type of condition was voluntarily created to produce significant spreading without excess natural splashing. In this study, fragmentation was achieved via the complementary effect of temperature and vibration.

Like J. Dewitte [12] demonstrated in the past, this study provides a  $T^* \cdot \log K'$  diagram of the impact conditions to account for the effect of temperature, where  $K'$  represents the Walzel number defined by (6) and  $T^*$  represents the reduced temperature defined by (7) in which  $T_w$ ,  $T_{eb}$  and  $T_{leid}$  respectively represent the surface temperature, the boiling point of the liquid, and its Leidenfrost temperature under the conditions obtained by extrapolating Figure 5. The boundaries indicating the appearance of splashing and rebound are recalled in [12]. The choice of the dimensionless number  $K'$  is justified by the fact that it covers the characteristics of the liquid and the dynamics of the impact.

$$K' = We \cdot Oh^{-0.4} \quad (6)$$

$$T^* = \frac{T_w - T_{eb}}{T_{leid} - T_{eb}} \quad (7)$$

Figure 14 makes it possible to position the impact conditions under investigation. In terms of the objective of this study which involves obtaining controlled secondary fragmentation, the rebound conditions have been proscribed by setting rather high  $K'$  values (thus Weber or Oh) while avoiding to impose too high temperatures on the surface. Furthermore, in the case of uranyl nitrite or PVA, the initial condition of the surface may change if the impact surface is heated excessively. This is due to the formation of a solid deposition resulting from the evaporation or decomposition of the liquid, which is penalising and thus must be limited.

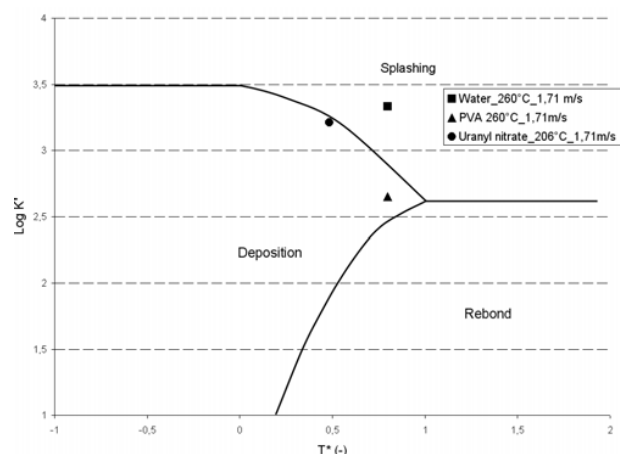


Fig. 14: Impact conditions on the surface as a function of the reduced temperature of the surface

### C. Secondary fragmentation

As previously mentioned, our research is aiming to achieve controlled fragmentation, i.e. not only due to natural splashing, but especially through the application of vibration capable of fragmenting the fingers produced during spreading. As previously shown (see Fig. 14), the number  $N$  of fingers does not seem to be strongly impacted by the application of vibrations under the tested conditions, though these vibrations do allow for secondary fragmentation which cannot occur otherwise, as shown in Figure 15. The main secondary droplets resulting from the fragmentation of the fingers by vibration tend to have diameters that are characteristic of the finger widths. In one case however (no vibration, see Fig. 14b), the fingers end up being reabsorbed due to the surface tension force, whereas the fingers are segmented into droplets when vibration is applied in compliance with the objective of this study which is to make microspheres. Figure 15 shows a zoom of a PVA/water solution which has a significantly higher viscosity than water. Despite this fact, the vibrations do have an impact. Generally speaking, the secondary droplets do not have a mono-dispersed grain size as shown in Figure 17 and Table IV.

TABLE IV  
GRANULOMETRY OF SECONDARY DROPLETS AFTER A DROP IMPACTING ON HEATED VIBRATED SOLID SURFACE (80 Hz,  $v=1.71$  m/s,  $T=265^\circ\text{C}$  water)

$\overline{D}_s$ (μm)	Ratio $D_s/D_o$ (%)	Ratio $V_s/V_o$ (%)	Amount (%)
205	5%	0,01	30
415	10%	0,10	20
995	24%	1,38	20

$\overline{D}_s$ : mean diameter of the secondary droplets after drop impact ; amounts are given taking into account the three main types of secondary droplets obtained after impact

$V_o$  and  $V_s$ : respectively the volume of the initial drop and droplets after secondary fragmentation



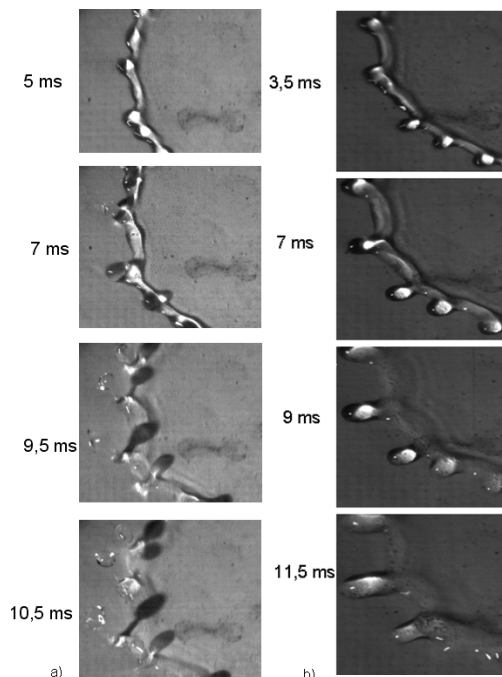


Fig. 15: Secondary fragmentation controlled by vibration of the surface impact after the spreading of a drop. ( $f = 80$  Hz ;  $T = 260^\circ\text{C}$ ,  $Re = 7300$ ) ; in Fig b), the spreading in the same conditions without vibration which does not break up the fingers

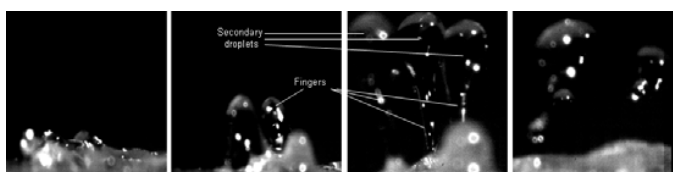


Fig. 16: Fragmentation of fingers by applying vibration (80 Hz) during the impact of a PVA/water droplet on a silicone surface heated to  $260^\circ\text{C}$   $Re \sim 150$

Following gelation of these secondary droplets (by making them fall into a solution of ammonia, see Fig. 8), spherical particles of polydispersed uranium oxide can be obtained (see Fig. 18) some of which are relatively small and will not block the injectors, thus meeting the objective of this study. Furthermore, the resulting velocities of the droplets due to vibration-assisted secondary fragmentation are relatively low, which is also an advantage when it comes to controlling the sphericity of the particles during droplet impact in the ammonia bath.

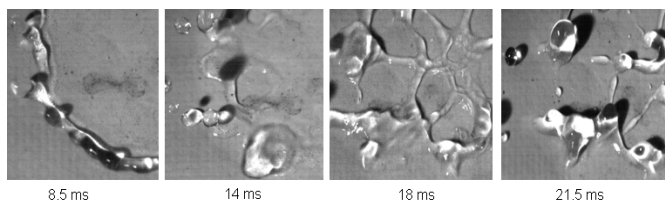


Fig 17: Fragmentation controlled by vibration on a heated vibrated solid surface for the case of a water drop impacting a vibrated (80 Hz) heated ( $260^\circ\text{C}$ ) surface

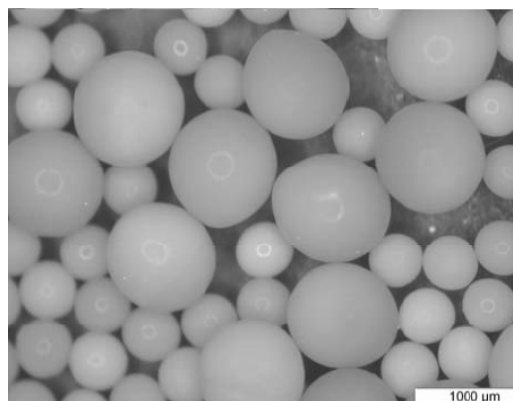


Fig. 18: Microspheres of uranium oxyde after gelation of droplets of uranyl nitrate

## VI. CONCLUSION

In this paper, the fragmentation of secondary droplets on a heated, vibrating surface was successfully achieved to produce small spherules of nuclear fuel, which thus rules out the risk of blockage in the injectors typically used for this type of operation. This novel method was implemented with water and PVA for reasons of simplicity, before being adapted for uranyl nitrate so as to consolidate the feasibility of the technique for the nuclear industry.

Secondary fragmentation is indeed favoured by the application of vibrations compared with a vibration-free situation. Furthermore, most of the secondary droplets, under the tested conditions, have a grain size similar to the characteristics of the fingers generated by natural impact, i.e. without vibration. It should nevertheless be pointed out that other secondary droplets have grain sizes that are both larger and smaller than those with a similar size to that of the fingers. Studies need to be pursued to optimise the main parameters governing the characteristics of the secondary droplets, such as the temperature of the impact surface, the vibration frequency, and the quantity of droplet movement prior to impact (a parameter that, in principle, increases the number of fingers and thus decreases the size of the droplets resulting from secondary fragmentation). Nonetheless, it already seems possible to imagine controlling the grain size of these droplets (and thus the resulting spherules following gelation) with simple parameters and within a range (i.e.  $< 100 \mu\text{m}$ ) that has so far been out of reach for standard injectors due to the risk of blockage.

## ACKNOWLEDGMENTS

The authors would like to thank A. Benedetti for his technical support on video data acquisition.

## REFERENCES

- [1] S.M. Tiegs, P.A. Haas, and R.D. Spence, "The Sphere-Cal Process : Fabrication of Fuel Pellets from Gel Microspheres", *ORNL/TM-6906*.



- [2] R.L. Beatty, R.E. Norman, and K.J. Notz, "Gel-Sphere-Pac Fuel for thermal Reactors – Assessment of fabrication Technology and Irradiation Performance", *ORNL-5469* (Nov. 1979).
- [3] R. Spence, "Sol Gel Spherical Fuel, Conf on metallurgical techn. of uranium and uranium alloys", *American Society for metals* (1981).
- [4] P. Naefe, and E. Zimmer, "Preparation of  $\text{UO}_2$  kernels by an external gelation process", *Nuclear Technology*, V. 42 (1979).
- [5] Patent GB2094771.
- [6] M.R. Simpson, C.Z. Stockwell, "Improvements in or relating to gelation", patent GB 1401962 (1 August 1975).
- [7] C.H.R. Mundo, M. Sommerfeld, and C. Tropea, "Droplet-wall collisions: experimental studies of the deformation and breakup process", *Int. J. Multiphase Flow* Vol. 21 n°2, 1995.
- [8] N. Zainoun, J-M Chicheportiche, J-P. Renaudeaux, "le vibro-générateur d'aérosols homogènes", *Proceedings of the annual conference ASFERA*, dec 2004.
- [9] A.L. Yarin, "Drop impact dynamics: splashing, spreading, receding, bouncing", *Annual Review of fluid mechanics*, vol. 38, 2006.
- [10] M. Bussmann, S. Chandra, and J. Mostaghimi, "Modeling the splash of a droplet impacting a solid surface, Physics of fluids", Vol.12, n°12, 2000.
- [11] M. Rein, "Phenomena of liquid drop impact on solid and liquid surfaces", *Fluid Dynamics Research*, 12 (1993) 61-93.
- [12] J. Dewitte, "Modelisation de l'impact d'un brouillard de gouttes en évaporation et sous pression sur une paroi chauffée", Thesis of PhD, 2006.
- [13] K.J. Baumeister, F.F. Simon and R.E. Henry, "Role of the surface in the measurement of the Leidenfrost temperature, Augmentation of Convective Heat and Mass Transfer", *ASME*, pp. 91-101, 1970.
- [14] L. Bolle and J.C. Moureau, "Spray cooling of hot surfaces, in Multiphase Science and Technology" (ed. By G.F. Hewitt, J.M. Delhay and N. Zuber) pp. 1-92. Hemisphere, New York, 1976.
- [15] H.Y. Kim, Z.C. Feng, and J.H. Chun, "Instability of a liquid jet emerging from a droplet upon collision with a solid surface", *Physics of fluids*, vol. 12, number 3, march 2000.
- [16] M.H. and J.C. Chen's., J.C. Chen, "Behavior of a liquid droplet impinging on a solid surface". *ASME*. 83-WA/HT-104
- [17] F. Akao, K. Araki, S. Lori and A. Moriyama, "Deformation behaviors of a liquid droplet impinging onto hot metal surface", *Trans. Int. Steel Inst. Japan* 20, 737-743 (1980)
- [18] M. Kurokawa and S. Toda, "Heat Transfer of an impacted single droplet on the wall", in *Proceedings of the ASME/JSME, Thermal Engineering Joint Conf*, Vol. 2, pp 141-146, 1991
- [19] A.L. Biance, F. Checy, C. Clanet, G. Lagubeau, D. Quere, "On the elasticity of an inertial liquid shock", *Journal of Fluid Mechanics* 554 (2006) 47-66
- [20] R. Bhola and S. Chandra, "Parameters controlling solidification of molten wax droplets falling on a solid surface", *J. Mater. Sci.* 34, 4883 (1999)
- [21] G.E. Cossali, A. Coghe, and M. Marengo, "The impact of a single drop on a wetted solid surface", *Exp. Fluids* 22, 463